RSC Advances

PAPER

View Article Online
View Journal | View Issue

Cite this: *RSC Adv.*, 2020, **10**, 35185

P-stereocontrolled synthesis of oligo(nucleoside N3′→O5′ phosphoramidothioate)s – opportunities and limitations†‡

Ewa Radzikowska, *[a] Renata Kaczmarek, [a] Dariusz Korczyński,[a] Agnieszka Krakowiak, [a] Barbara Mikołajczyk,[a] Janina Baraniak,[a] Piotr Guga, [a] Kraig A. Wheeler, [b] Tomasz Pawlak [a] and Barbara Nawrot [a]

3′-*N*-(2-Thio-1,3,2-oxathiaphospholane) derivatives of 5′-*O*-DMT-3′-amino-2′,3′-dideoxyribonucleosides ($_N$OTP-N), that bear a 4,4-unsubstituted, 4,4-dimethyl, or 4,4-pentamethylene substituted oxathiaphospholane ring, were synthesized. Within these three series, $_N$OTP-N differed by canonical nucleobases (*i.e.*, Ade^{Bz}, Cyt^{Bz}, Gua^{iBu}, or Thy). The monomers were chromatographically separated into P-diastereomers, which were further used to prepare $N_{NPS}N'$ dinucleotides (**3**), as well as short P-stereodefined oligo(deoxyribonucleoside N3′→O5′ phosphoramidothioate)s (NPS-) and chimeric NPS/PO- and NPS/PS-oligomers. The condensation reaction for $_N$OTP-N monomers was found to be 5–6 times slower than the analogous OTP derivatives. When the 5′-end nucleoside of a growing oligomer adopts a C3′-*endo* conformation, a conformational 'clash' with the incoming $_N$OTP-N monomer takes place, which is a main factor decreasing the repetitive yield of chain elongation. Although both isomers of $N_{NPS}N'$ were digested by the HINT1 phosphoramidase enzyme, the isomers hydrolyzed at a faster rate were tentatively assigned the R_P absolute configuration. This assignment is supported by X-ray analysis of the protected dinucleotide $^{DMT}dG^{iBu}{}_{NPSMe}T_{OAc}$, which is P-stereoequivalent to the hydrolyzed faster P-diastereomer of $dG_{NPS}T$.

Received 5th June 2020
Accepted 15th September 2020

DOI: 10.1039/d0ra04987e

rsc.li/rsc-advances

Introduction

Therapeutic properties of synthetic DNA oligonucleotides (PO-oligos) targeted against complementary DNA or mRNA molecules have been tested for more than 40 years.[1] In principle, the probes should be characterized by high target affinity, efficient cellular uptake, and enhanced resistance towards nucleases. To make PO-oligos more stable towards nucleases, phosphorothioate analogs (PS-oligos, a dinucleotide $N_{PS}N'$ (**1**) is shown in Chart 1) were introduced many years ago[2] and remain of interest to the scientific community today.[2e] A single PO→PS substitution performed with a non-bridging oxygen atom produces a new stereogenic center, thus PS-oligos synthesized by the standard, marginally stereoselective, phosphoramidite or H-phosphonate methods are mixtures of hundreds or thousands of P-diastereomers.[3] To date, P-stereodefined PS-oligos have been mainly prepared by (developed in this laboratory) the oxathiaphospholane approach[4] (Otp, see Scheme 1) based on the use of P-diastereomerically pure 5′-*O*-DMT-nucleoside-3′-*O*-(2-thio-1,3,2-oxathiaphospholane)s or their 4,4-disubstituted analogs (OTP-N; R = H or R = Me or R,R = $-(CH_2)_5-$, Scheme 1). Other methods are available as well.[5] With the exception of homopurine R_P-PS-oligos, which with the RNA complement(s)

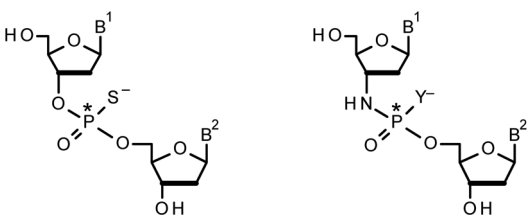

1, $N_{PS}N'$, PS-oligo

2, Y = O ($N_{NP}N'$, NPO-oligo)
3, Y = S ($N_{NPS}N'$, NPS-oligo)

Chart 1 B^1,B^2 = Ade, Cyt, Gua or Thy. The asterisks indicate the P-stereogenic centers.

[a]*Centre of Molecular and Macromolecular Studies, Polish Academy of Sciences, Sienkiewicza 112, 90-363 Łódź, Poland. E-mail: eradziko@cbmm.lodz.pl*
[b]*Whitworth University, Department of Chemistry, 300 W. Hawthorne Rd., Spokane, WA, 99251, USA*

† Dedicated to Prof. Dr Wojciech J. Stec on the occasion of his 80th birthday.

‡ Electronic supplementary information (ESI) available: HR MS, ^{31}P NMR, ^{1}H NMR, and ^{13}C NMR spectra of separated P-epimers of **4–6**; MS and ^{31}P NMR data for unresolved monomers **4–6**; ^{31}P NMR, ^{1}H NMR, ^{13}C NMR spectra, details of crystallographic analysis, and crystal structure of $^{DMT}dG^{iBu}{}_{NPSMe}T_{OAc}$ obtained from **6Gf**; selected data for NPS- and chimeric NPS/PO oligomers. CCDC 1939477. For ESI and crystallographic data in CIF or other electronic format see DOI: 10.1039/d0ra04987e

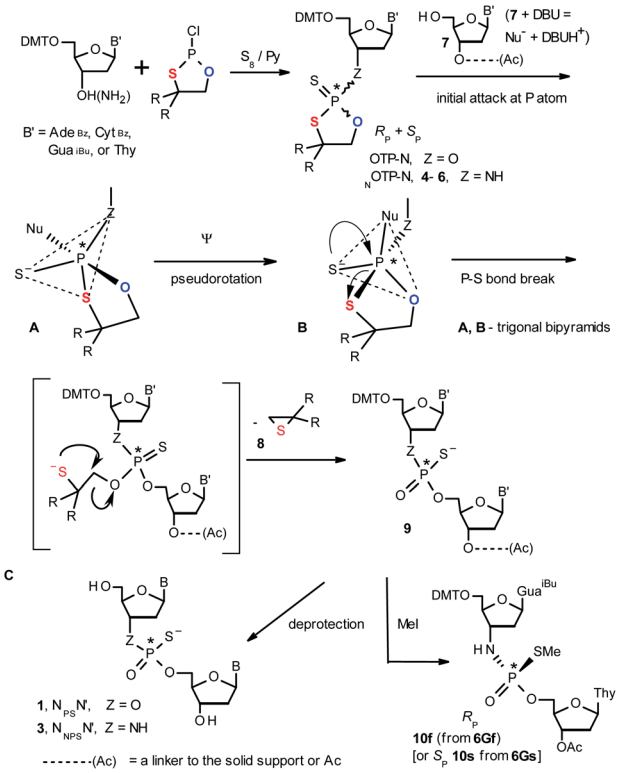

Scheme 1 A mechanism of the DBU-promoted condensation step in Otp synthesis of $N_{PS}N'$ or $N_{NPS}N'$ with the use of a mixture of P-epimers of OTP-N (Z = O) or $_N$OTP-N monomers (Z = NH), respectively. **4**, R = H; **5**, R = Me; **6**, R,R = $-(CH_2)_5-$. B′ = Ade^{Bz}, Cyt^{Bz}, Gua^{iBu}, or Thy. The codes **6Gf** and **6Gs** indicate fast- and slow-eluting P-diastereomers of *Pm*-$_N$OTP-dG (*vide infra*).

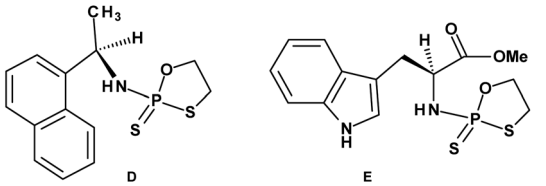

Chart 2 (D) (R_c)-2-(1-(α-Naphthyl)ethyl)amino)-2-thio-1,3,2-oxathiaphospholane, (E) a 2-thio-1,3,2-oxathiaphospholane derivative of L-tryptophan methyl ester; $_N$OTP-Trp.

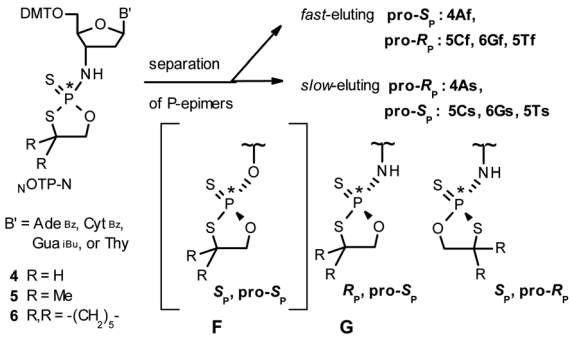

Scheme 2 Effects of silica gel separation of P-diastereomers of 2-thio-1,3,2-oxathiaphospholane monomers **4–6**. The descriptors pro-R_P and pro-S_P indicate the absolute configuration of P-atom in the subsequently formed internucleotide phosphoramidothioate linkages. The structure **F** is given only for comparison with **G**.

form thermally stable parallel duplexes and triplexes with overall A conformation,[6] both R_P- and S_P-PS-oligos possess unfavorable hybridization properties as compared to those observed for the unmodified oligonucleotides.[7] However, their physico-chemical[7–9] and biological[10–12] properties often depend on the absolute configuration of the P-atoms.

Another class of DNA analogs of considerable nucleolytic stability consists of P-achiral oligo(deoxyribonucleoside phosphoramidate)s[13] (NPO-oligos, a dinucleotide $N_{NP}N'$ (**2**) is shown in Chart 1), in which the 3′-oxygen atom is replaced by a nitrogen atom.[14] CD measurements[15] as well as high-resolution X-ray crystallographic data[16] of duplexes formed by NPO-oligos and DNA or RNA strands revealed A-like conformations, which contribute to their high thermal stability.[15] NPO-oligos were found to be allosteric inhibitors of telomerase, which is a ribonucleoprotein responsible for maintaining telomeres in nearly all eukaryotic cells.[17]

Oligo(deoxyribonucleoside phosphoramidothioate)s (NPS-oligos, a dinucleotide $N_{NPS}N'$ (**3**) is shown in Chart 1 and in Scheme 1) were synthesized to combine the useful properties of PS- and NPO-oligos.[18] NPS-oligos are P-chiral and the syntheses based on the widely used, yet of low stereoselectivity, phosphoramidite or H-phosphonate methodology generate stereorandom mixtures of P-epimers. Important biochemical findings about NPS-oligos§ prompted us to check if P-stereodefined NPS-oligos may be obtained in a variant form of the Otp methodology using the monomers **4–6** ($_N$OTP-N, Z = NH: **4**, R = H; **5**, R = Me; **6**, R,R = $-(CH_2)_5-$; B′ = Ade^{Bz}, Cyt^{Bz}, Gua^{iBu}, or Thy, Scheme 1). Importantly, it was documented,[19] that if Z = O the Otp condensation does not follow a stereoinvertive S_N2P mechanism, but this is a stereoretentive process, where the initial attack of a nucleophile **7** takes place from the side opposite to the most electronegative atom attached to the phosphorus center (the oxygen atom in OTP-N, marked in blue; Scheme 1) to form a trigonal bipyramid **A**. Then, the permutational isomerization (a pseudorotation process) furnishes the bipyramid **B**, where the leaving thioalkyl group occupies the axial position, necessary for the cleavage of the P–S bond. The condensation process concludes with the elimination of episulfide **8** from the triester intermediate **C**. It was assumed, that $_N$OTP-N would react with the 5′-OH group of **7** in an analogous manner to yield phosphoramidothioate diester **9** (Z = NH), with a final deprotection step producing NPS-oligos **3**.

Early studies in this field showed that both P-epimers of (R_c)-2-(1-(α-naphthyl)ethyl)amino)-2-thio-1,3,2-oxathiaphospholane (Chart 2, structure **D**) in the presence of DBU reacted with primary alcohols to give products with stereochemical retention

§ Noteworthy, an NPS-oligomer bearing a lipid tag (GRN163L[50]) was found to be a potent inhibitor of human telomerase,[51] which is an enzyme highly active in ~85% of known human tumor cells, whereas in normal cells its activity is marginal.

Table 1 Characteristics of separated P-diastereomers of $_N$OTP-N **4–6**

B′, R,R	Yield[a] (%)	MW calc. (Da)	TOF MS ES (*m*/*z*)[b]	Code	R_f[c]	^{31}P NMR[d] (δ, ppm)
Ade^{Bz}, H,H	83	794	795.2191; 817.2008 [M + Na$^+$] 100%	**4Af**[i]	0.50	95.92
	24/12[e]			**4As**[i]	0.48[j]	95.25
Cyt^{Bz}, Me,Me	79	798	799.2385	**5Cf**	0.70	97.74
	19/26[f]			**5Cs**	0.65[k]	97.25
Gua^{iBu}, –(CH$_2$)$_5$–	84	844	845.2920	**6Gf**	0.58	96.92
	52/26[g]			**6Gs**	0.47[k]	96.94
Thy, Me,Me	88	709	732.1951, [M + Na$^+$]	**5Tf**	0.65	96.69
	22/22[h]			**5Ts**	0.58[l]	96.58

[a] Total yield of the isolated mixture of isomers; yields of the separated fast- and slow-eluting isomers, respectively; 'flash' chromatography on silica gel 200–300 mesh was performed unless otherwise stated. [b] [M + H$^+$] ions, measured for the unresolved mixture of P-epimers. [c] HP TLC plates. [d] In $CDCl_3$. [e] Silica gel 60H, 0 → 1% MeOH/$CHCl_3$, v/v. [f] 0 → 2% MeOH/$CHCl_3$, v/v. [g] $CHCl_3$: MeOH 50 : 1, v/v. [h] AcOEt : hexane 1 : 1, v/v. [i] Only a minute amount of **4Af** was isolated and in further experiments a 1 : 2 mixture of **4Af** and **4As** was used. [j] $CHCl_3$: MeOH 20 : 1, v/v, double development. [k] $CHCl_3$: MeOH 20 : 1, v/v. [l] AcOEt : hexane 1 : 1, v/v.

– *i.e.*, the incoming alkoxyl group was found in the product at the position originally occupied by the endocyclic sulfur atom (marked in red in Scheme 1).[20]

Several years ago such high stereoselectivity was confirmed in the reaction of the $_N$OTP derivative of L-tryptophan methyl ester ($_N$OTP-Trp, Chart 2, structure **E**) with *O*2′,*O*3′,*N*6-tribenzoyl-adenosine[21] leading to the tribenzoylated derivative of AMPS-Trp-OMe. Similar stereoselective results were achieved from the reactions of P-diastereomers of the $_N$OTP derivative of 3′-amino-3′-deoxy-thymidine (**5**, B′ = Thy) with 3′-*O*-acetyl-thymidine, which (after deprotection) furnished the T$_{NPS}$T dimers.[22]

Once obtained, homopurine R_P-NPS-oligos with the anticipated intrinsic C3′-*endo* conformation (*vide supra*) could be used to effectively stabilize the previously described parallel duplexes and triplexes.[6]

Here we show that using P-diastereomerically pure $_N$OTP-N monomers results in P-stereodefined chimeric PO/NPS- or PS/NPS-oligos with the NPS-nucleotides introduced in "alternate" positions. Additional experiments revealed several structural factors responsible for the observed low repetitive yields in the solid phase synthesis of uniformly modified NPS-oligos.

Results and discussion

Preparation of P-diastereomerically pure $_N$OTP-N monomers 4–6

Our earlier experiments with OTP-N monomers (Z = O, Scheme 1) showed that in terms of chromatographic separability of P-diastereomers, those 4,4-unsubstituted (R = H) were most troublesome, followed by the more convenient compounds bearing R = Me and the most useful 4,4-pentamethylene substituted congeners.[4] The same was observed for their LNA (Locked Nucleic Acids) analogs.¶

In the present work three sets of $_N$OTP-N monomers (4,4-unsubstituted, *Un*-, **4**; 4,4-dimethyl substituted, *Dm*-, **5**; and 4,4-pentamethylene substituted, *Pm*-$_N$OTP-N, **6**; Scheme 2) were obtained from the 5′-*O*-DMT derivatives of 3′-amino-2′,3′-dideoxy-ribonucleosides. However, chromatographic separation of P-diastereomers was achieved only for **4A**, **5T**, **5C**, and **6G** (the suffixes **A**, **G**, **C** or **T** indicate the Ade, Gua, Cyt or Thy nucleobases, respectively). The chromatographic details related to the separation of the fast- and slow-eluting P-diastereomers are given in Table 1, and the relative mobility is reflected in their codes by an f or s suffix, respectively (*e.g.* **4Af** or **4As**, Scheme 2). The relevant HR MS, ^{31}P NMR, ^{1}H NMR, and ^{13}C NMR spectra are shown in Data Sets S1–S4 and Fig. S1–S4 (ESI).‡ Attempts to separate other $_N$OTP-Ns, *e.g.* **5A** or **6A**, were unsuccessful with the data for unresolved **4–6** given in Table S1 (ESI).‡ [Note: The pro-R_P and pro-S_P descriptors, shown in Scheme 2, indicate the absolute configuration of P-atom in the internucleotide phosphoramidothioate moiety formed upon condensation of a given P-diastereomer of $_N$OTP-N with the 5′-OH group of a nucleoside/nucleotide. The assignment was based on the differences in rates of hydrolysis of P-diastereomeric N$_{NPS}$N′ dinucleotides **3** (Scheme 1) with HINT1 phosphoramidase (*vide infra*)]. It should be noted, that stereochemically equivalent pro-S_P OTP-N and $_N$OTP-N monomers (Scheme 2, **F** and **G**, respectively) have opposite absolute configurations of the phosphorus stereogenic centers. Obviously, the same relationship is valid for the pro-R_P pairs.

Tentative assignment of the absolute configuration at P-atoms in separated diastereomers of $_N$OTP-Ns 4–6

During the course of earlier works on stereocontrolled synthesis of PS-oligos, the experiments of enzymatic hydrolysis of dinucleoside phosphorothioates N$_{PS}$N′ (**1**) with R_P-specific snake venom phosphodiesterase (svPDE) and S_P-specific Nuclease P1 (ref. 23) provided sufficient data to establish an empirical rule that the fast-eluting *Un*-OTP-N (Z = O, B′ = Ade^{Bz}, Cyt^{Bz}, Gua^{iBu,DPC}, or Thy) are precursors of S_P-N$_{PS}$N′, contrary to fast-eluting *Dm*- and *Pm*-OTP-N congeners, which yield R_P-N$_{PS}$-N′.[4a,19] This relationship was later confirmed for the *Pm*-OTP derivatives of LNA nucleosides.[24,25] Unfortunately, although NPO-oligos were hydrolyzed by svPDE to a measurable extent (after 4.5 h incubation ~50% of NPO-T$_{10}$ remained intact;[13a]

¶ Unpublished results. The rank was determined during work on ref. 25.

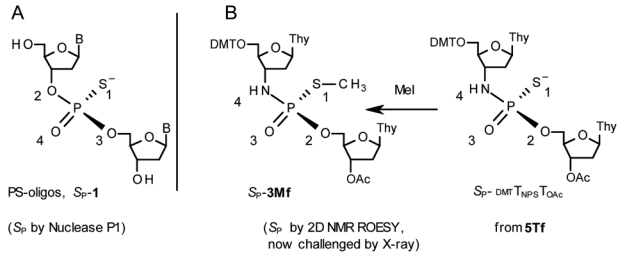

Chart 3 Orientation of the sulfur, phosphoryl oxygen and thymidine O5′ atoms around the phosphorus atoms: Panel A, in phosphorothioate S_P-**1**, ref. 23; Panel B, 2D NMR ROESY based assignment (here challenged by X-ray analysis of **10f**, Scheme 1) in the *S*-methylated S_P-**3Mf**, ref. 22 (the phosphoramidothioate diester precursor was obtained from fast-eluting **5Tf**). The Arabic numerals 1–4 indicate the priority of substituents around the phosphorus atoms according to the Cahn–Ingold–Prelog rules. Note: to establish the priority of substituents, the formal double bond between the phosphoryl oxygen atom and the phosphorus atom (P═O) should be considered a single one.

after 24 h incubation phosphoramidate $T_{NP}T$ was hydrolyzed in 22% yield, data not shown), phosphoramidothioates **3** when treated with svPDE or Nuclease P1 remained intact.

A few years ago, chromatographically separated **5Tf** and **5Ts** (R = Me, B′ = Thy) and 3′-*O*-acetylated thymidine were used in the synthesis of P-diastereomeric $^{DMT}T_{NPS}T_{OAc}$ (5′-*O*-DMT and 3′-*O*-Ac protected precursors of **3**, Chart 3).[22] Both anionic $^{DMT}T_{NPS}T_{OAc}$ diesters were then stereoretentively *S*-methylated to yield the corresponding P-diastereomeric triesters $^{DMT}T_{NPSMe}T_{OAc}$ (**3Mf** and **3Ms**, Chart 3). At that point, 2D NMR ROESY experiments suggested that, contrary to the aforementioned empirical rule, the relative orientation of the sulfur, phosphoryl oxygen and thymidine O5′ atoms around the phosphorus atom in the *S*-methylated triester **3Mf** (Chart 3, obtained from the fast-eluting **5Tf**) is equivalent to that in phosphorothioate S_P-**1**, which is hydrolyzed by Nuclease P1. Consequently, **3Ms** obtained from the slow-eluting **5Ts** is P-stereoequivalent to R_P-**1**, which is hydrolyzed by svPDE. Although the O3′→N3′ replacement does change the priority of substituents (O3′ – priority 2, N3′ – priority 4), by virtue of the formalism of the Cahn-Ingold-Prelog rules, not only the relative

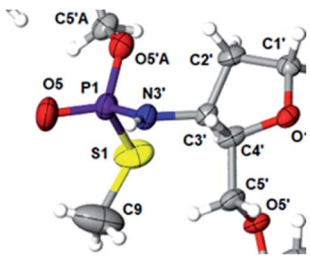

Fig. 1 Crystal structure of $^{DMT}dG^{iBu}{}_{NPSMe}T_{OAc}$ **10f** showing partial structure and spatial orientation of substituents around the phosphorus stereogenic center (marked P1). Compound **10** was obtained from the monomer **6Gf** (fast-eluting 5′-*O*-DMT-3′-amino-2′,3′-dideoxy-*N*6-iBu-guanosine-3′-*N*-(2-thio-4,4-pentamethylene-1,3,2-oxathiaphospholane). The oxygen atom marked O5′A belongs to the thymidine residue.

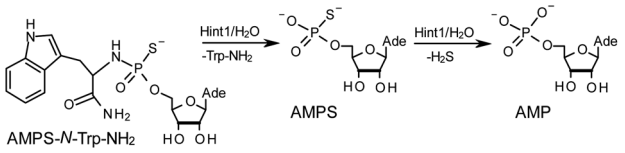

Scheme 3 The HINT1 catalyzed hydrolysis of adenosine-5′-*O*-((L-tryptophan amide-*N*α-yl)-phosphoramidothioate) (AMPS-Trp-NH_2), followed by desulfuration of the AMPS intermediate leading to the formation of adenosine-5′-*O*-phosphate.

orientations but also the absolute configurations of P atoms in S_P-**1**, and **3Mf** are the same.

This violation of the empirical rule "fast-eluting *Dm*- and *Pm*-OTP-N → R_P-N_{PS}N" could not be explained by the C3′-*endo* conformation of the sugar moiety in 3′-amino-2′,3′-dideoxynucleosides, because the C3′-*endo* locked LNA-derived oxathiaphospholane monomers adhere to that rule.[24] In the present work, this unexpected NMR-based assignment was challenged by a successful crystallographic experiment, which showed the rule-obeying R_P absolute configuration (Fig. 1) for a non-ionic $^{DMT}dG^{iBu}{}_{NPSMe}T_{OAc}$ amidodiester (**10f**, Scheme 1, ESI‡) obtained from the fast-eluting **6Gf** (a *Pm*-derivative) after S-methylation of the negatively charged amidoester intermediate $^{DMT}dG^{iBu}{}_{NPS}T_{OAc}$ (**9**). Importantly, compound **10f** crystallized spontaneously, without the typically applied slow evaporation. The complete crystal structure is shown in Fig. S7 (ESI)‡ with crystallographic details summarized in Table S2 (ESI).‡

The opposite absolute configurations of P-atoms determined by the dinucleotide derivatives **3Mf** and **10f**, obtained from the fast-eluting *Dm*-**5Tf** (the NMR data) and from the fast-eluting *Pm*-**6Gf** (the X-ray data), respectively, seemed to be a contradiction. Although it is possible that the *Dm*-$_N$OTP monomers, unlike *Dm*-OTP monomers, behave differently from the *Pm*-analogs, the contradiction could not be left unaddressed. Because attempts at crystallization of other $N_{NPS}N'$ dimers (protected or unprotected) or their $_N$OTP-N precursors were unsuccessful, we turned our attention to HINT1 phosphoramidase. This enzyme belongs to a family of hydrolases and transferases characterized by the presence of the histidine triad H–X–H–X–H–X–X–X (HIT) motif at their catalytic center, where H is a histidine residue and X is a hydrophobic amino acid.[26] The HINT1 catalyzed *in vitro* hydrolysis of the P–N bond releases (d)NMP or (d)NMPS from their phosphoramidate or phosphoramidothioate conjugates with amino acids, *e.g.*, from a conjugate of L-tryptophan amide and AMPS (AMPS-Trp-NH_2‖, Scheme 3).[21,27]

It is known that the hydrolysis of the P–N bond in the R_P isomer of AMPS-Trp-NH_2 is approximately 4 times faster than the same reaction using the S_P counterpart.[21] The released (d)NMPS is further desulfured to form (d)NMP and hydrogen sulfide, and this secondary nucleotide product must be taken into account during HPLC-based quantification of the products

‖ AMPS-Trp-NH_2 was concomitantly obtained from AMPS-Trp-OMe during ammonolysis of the protecting benzoyl groups in the adenosine moiety.

Table 2 Coupling yields [%] in solid phase synthesis of the NPS-dimers **11–17** calculated from the DMT^+ cation measurement. The descriptions fast and slow refer to the relative chromatographic mobility of $_N$OTP-N monomers

		$_N$OTP-N substrate	
$_N$OTP-N	d($N_{NPS}N'$)	Fast	Slow
4A	**11** d($A_{NPS}A$)		73[a]
5C	**12** d($C_{NPS}A$)	98	95
6G	**13** d($G_{NPS}G$)	75	46
5T	**14** T_{NPS}dA	93	89
5T	**15** T_{NPS}dG	98	95
5T	**16** T_{NPS}T	99	96
6G	**17** dG_{NPS}T	84	69

[a] For a 1 : 2 mixture of **4Af** and **4As**, see note *i* to Table 1.

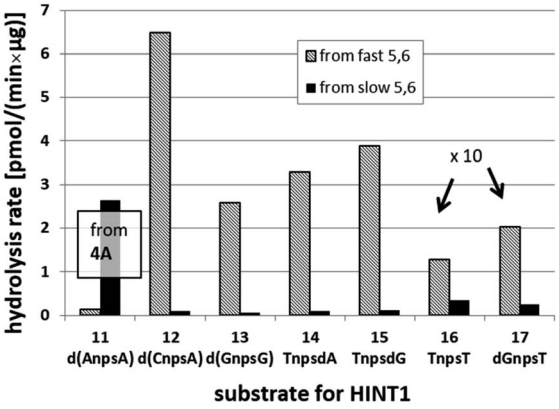

Fig. 2 Rates of hydrolysis of NPS-dinucleotides **11–17** (data from Table 2). The descriptions fast and slow refer to the relative chromatographic mobility of $_N$OTP-N precursors. For better visualization the heights of bars depicting the rates of hydrolysis of **16** and **17** have been scaled up by a factor of 10.

of hydrolysis. The rates of desulfuration of (d)NMPS decrease in the following order: AMPS, GMPS ≥ CMPS > UMPS > dAMPS, dGMPS >> dCMPS, TMPS.[28] One can assume that this decreasing order of affinity would also be reflected in the rates of hydrolysis of the R_P and S_P series of (d)NMPS-conjugates. To determine the absolute configuration at P-atoms in the oligomers obtained from the separated fast- and slow-eluting P-diastereomers of **4–6**, model $N_{NPS}N'$ dimers **11–17** (see Table 2) were prepared using the solid phase synthesis method. Due to the small difference of R_f values, only a minute amount of **4Af** was isolated and in further experiments a 1 : 2 mixture of **4Af** and **4As** was used. [Notes: (a) To prevent the DBU-promoted intramolecular cleavage of the standard LCAA (long chain alkylamino) linker, a modified solid-phase support (-$) was used, in which the 3′-OH group of nucleoside was attached to the CPG (controlled pore glass) beads *via* a sarcosine linker [–$COCH_2CH_2CON(CH_3)CH_2CO$–LCAA–CPG].[29] (b) To assess relative reactivity of $_N$OTP-N and OTP-N monomers, ^{HO}dG-**$** was elongated with an equimolar mixture of $_N$OTP-T and OTP-T, and the resultant mixture consisted of T_{NPS}dG and T_{PS}dG at *ca.* 1 : 5 ratio.]

We recognized that the d($N_{NPS}N'$) dimers, as well as T_{NPO}T, were hydrolyzed by recombinant human HINT1 phosphoramidase. In an initial rate assay, the substrates were treated at 37 °C until 10% degradation was detected by RP HPLC. The observed hydrolysis rates are given in Fig. 2 and Table 3. [Note: because the phosphoramidate conjugates of TMPS are the least effective substrates for HINT1 (*vide supra*) the rates of hydrolysis of **16** and **17** were very low; therefore, for better visualization the corresponding four bars in Fig. 2 were increased by a factor of 10.] Assuming that the hydrolysis of $N_{NPS}N'$ mechanistically follows that observed for AMPS-Trp-NH_2, the R_P-$N_{NPS}N'$ dimers should be hydrolyzed faster than the S_P counterparts. Based on this assumption, the HPLC analysis allowed assignment of the R_P absolute configuration to d($A_{NPS}A$) obtained from slow-eluting **4As**, and to d($C_{NPS}A$), T_{NPS}dA, T_{NPS}dG, T_{NPS}T, dG_{NPS}T, and d($G_{NPS}G$) obtained from fast-eluting **5Cf**, **5Tf**, and **6Gf**. This conclusion is contradictory to the earlier assignment from NMR data, but is consistent with the result of X-ray analysis shown in Fig. 1. Since the NMR based assessment of absolute configuration is less reliable than the crystallographic analysis, we claim that the resolved $_N$OTP-N monomers follow the earlier observations made for OTP-N, so the fast-eluting **4Af** is a precursor of S_P-$N_{NPS}N'$, and fast-eluting *Dm*- and *Pm*-$_N$OTP-N yield R_P-$N_{NPS}N'$.

Factors affecting the yield of condensation using $_N$OTP-N

The previous experiments performed in our laboratory showed that, although the yield of the first coupling step of **6T** (a mixture of P-diastereomers) with the 5′-OH group of a deoxyribonucleoside attached to a solid support was acceptable (*ca.* 90%), the yields associated with the subsequent coupling steps decreased at least by half.[30] No improvement was observed when longer reaction times (600 s) or double delivery of the

Table 3 Hydrolysis rates [pmol (min × µg protein)$^{-1}$] found in the HINT1 catalyzed cleavage of the $N_{NPS}N'$ **11–17** and the reference T_{NPO}T (the initial rate assay). The descriptions fast and slow refer to the relative chromatographic mobility of the starting $_N$OTP-N monomers. Each value represents the mean ± SD from at least three measurements

		$_N$OTP-N substrate	
$_N$OTP-N	d($N_{NPS}N'$)	Fast	Slow
4A	**11** d($A_{NPS}A$)[a]	0.135 ± 0.007	2.65 ± 0.30
5C	**12** d($C_{NPS}A$)	6.48 ± 0.36	0.107 ± 0.025
6G	**13** d($G_{NPS}G$)	2.585 ± 0.019	0.063 ± 0.007
5T	**14** T_{NPS}dA	3.296 ± 0.631	0.099 ± 0.010
5T	**15** T_{NPS}dG	3.883 ± 0.651	0.125 ± 0.023
5T	**16** T_{NPS}T	0.129 ± 0.160	0.034 ± 0.007
6G	**17** dG_{NPS}T	0.202 ± 0.044	0.026 ± 0.004
NA	T_{NPO}T	7.171 ± 1.225	

[a] Because a 1 : 2 mixture of **4Af** and **4As** was used in synthesis of **11**, the corresponding 1 : 2 mixture of P-diastereomers was formed and P-diastereomerically pure **11** were obtained by RP HPLC separation of the fully deprotected compounds.

monomer (the second delivery after washing and drying of the support) were applied.

Solvent-related factors. We decided to assess whether this failure was caused by poor solvation of the growing anionic $^{HO}N_{NPS}N'$… oligomer in aprotic CH_3CN, resulting in its poor "solubility" and restricted accessibility of the 5′-OH group (the reacting nucleophile) for the reagents. In an attempt to improve the solvation we used highly polar DMF, although this co-solvent did not help when the 2-oxo-4,4-pentamethylene-1,3,2-oxathiaphospholane analog of **6T** was used in the synthesis of NPO-oligos.[30] Unfortunately, when ^{HO}dG-**$** or ^{HO}d($G_{NPS}$G)-**$** were elongated with $_N$OTP-dG (**6G**) in a CH_3CN/DMF mixture (6 : 4, v/v) the condensation yield dropped even more (25–30%, assessed by the DMT^+ assay, Fig. 3, Exp. #1), whereas the condensation with OTP-N (R = H) in the same solvent mixture was >90% effective (data not shown).

Because chemically NPS-oligos and PS-oligos differ by the presence of a 3′-NH amide group (a potent donor of hydrogen bonding) instead of 3′-O ester atom (a weak acceptor), one might assume that the former may be involved in aggregation, which potentially may be disrupted by the coordination of the 3′-NH with a strong non-nucleophilic amine. Because DBU is a sterically hindered amine and perhaps unable to provide this coordination, we tried to use a mixture of DBU and other less sterically demanding amines. The coupling reactions were performed at the 1 μmol scale (in all experiments thymidine was attached to the support) using 20-fold molar excess of each of four $_N$OTP-N monomer **4**, 50-fold excess of DBU and, starting from the second coupling, 50-fold excess of the additional amine. Unexpectedly, we noted a significantly increased repetitive yield of condensation only for **4T** (67–88%, assessed by the DMT^+ cation assay, Table 4). For unknown reasons, the best and the worst results were obtained using NEt_3 and structurally similar NBu_3, respectively. It should be noted that although in the past triethylamine was found to promote the condensation of much more reactive OTP-N monomers, the rate of coupling was low and several hours were necessary to complete the process.[19]

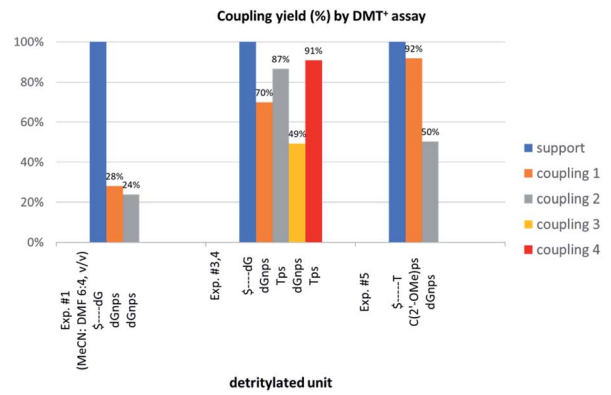

Fig. 3 Coupling yields in the consecutive condensation steps, assessed by DMT^+ assay at 504 nm. Absorptions of the DMT^+ cation released from the nucleosides attached to the support (blue bars) are taken as 100%.

Table 4 Repetitive yield of coupling and overall yield of manual solid-phase synthesis (at 1 μmol scale) of the $T_{NPS}T_{NPS}T_{NPS}T$ oligomer using a monomer **4T** and a mixture of DBU and given amine. The yields are derived from the DMT^+ cation assay

Amine	pK_a	Repetitive yield (%)	Overall yield (%)
NBu_3	10.89	67	33
NEt_3	10.76	88	68
DIPEA	10.50	76	44
DMAP	9.20	78	48
Collidine	7.48	74	36

Table 5 Average yield of the two consecutive coupling steps (%) in synthesis of $N_{NPS}N_{NPS}N$ utilizing the unresolved $_N$OTP-N monomers of different type

	Nucleobase			
$_N$OTP-N	Ade^{Bz}	Cyt^{Bz}	Gua^{iBu}	Thy
4	78	86	84	88
5	21	71	63	81
6	8	60	40	66

Conformation-related factors. Data provided in Table 2 indicate that the first condensations with a solid support bound DNA nucleoside proceeded with required 90+% efficacy only for pyrimidine monomers **5T** and **5C**, while **6G** offered the lowest coupling yield with, both T and dG bound to the support.** To gain a more general understanding of this process, we extended this assay to all synthesized monomers, although the unresolved mixtures of P-diastereomers were used and coupling conditions were not optimized. In principle, these tendencies are seen for all investigated $_N$OTP-N (Table 5), *i.e.*, the pyrimidine monomers are more reactive than purine ones.

Additionally, increasing the steric bulk of C4 substituents on the oxathiaphospholane ring results in a decrease in coupling efficiency. This phenomenon was most profound for **4A**, **5A**, and **6A**, and using **6A** the trimer d($A_{NPS}A_{NPS}A$) was obtained in less than 10%. Fortunately, much more reactive **4A** can be resolved onto P-epimers. On the contrary, **4G** and **5G** are much more reactive than **6G**, but only the epimers of the latter monomer (**6Gf** and **6Gs**) are separable. Interestingly, there are significant differences in the coupling yields for **6Gf** and **6Gs** (Table 2, 75% *vs.* 46%, 84% *vs.* 69%) and this observation prompted us to perform some calculations (using a Gaussian 16 software (ref. 31)) to assess their geometries. As expected, it was found that both compounds predominantly exist in a C3′-*endo* conformation. Then we focused our attention on the accessibility of the phosphorus centers for the initial attack of the nucleophile

** It must be pointed out that all the supports used were loaded with a given nucleoside to a similar extent (29–33 μmol g^{-1}), and before the first condensation the support was extensively capped (Ac_2O/DMAP/2,6-lutidine/tetrahydrofuran) to exclude unspecific coupling.

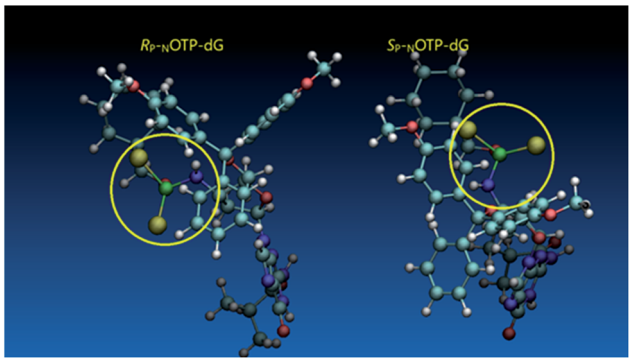

Fig. 4 Visualization of the lowest energy conformers of **6G** (R_P *Pm*-$_N$OTP-dG and S_P *Pm*-$_N$OTP-dG). The data were obtained using the Gaussian 16 package. Heteroatom labeling: P-green, O-red, S-yellow, N-navy blue.

leading to the formation of the bipyramid **A** (Scheme 1). The views along the P–O bonds (the P and O atoms are green and red, respectively) are presented in Fig. 4. Comparing the areas inside the yellow circles one can notice that the steric hindrance is much lower in S_P $_N$OTP-dG, so the more reactive **6Gf** can be tentatively assigned the S_P absolute configuration. Consequently, **6Gf** should be a precursor for R_P-$N_{NPS}N'$ dinucleotides. This assignment is consistent with the crystallographic data collected for **10f** and with the results of Hint1 promoted hydrolysis of **13** and **17**, but cannot be considered decisive.

Working earlier with LNA-derived OTP monomers (OTP-N^{LNA}, which adopt the profound C3′-*endo* conformation), we observed (Exp. #2) that in the synthesis of per-(PS-LNA) oligonucleotides even double condensation of OTP-N^{LNA} to $^{HO}N^{LNA}{}_{PS}$…-**$** was ineffective and a DMT^+ cation absorption virtually decayed after the 5th cycle (K. Jastrzębska, P. Guga, unpublished data); whereas, such a condensation with the 5′–OH–DNA-**$** proceeded with >94% efficacy.[24] As mentioned earlier, molecular modeling showed that poorly reacting **6Gf** and **6Gs** predominantly exist in a C3′-*endo* conformation. To verify whether the most reactive $_N$OTP-T monomers **5Tf** and **5Ts** adopt that conformation (characteristic of 3′-amino-2′,3′-dideoxyribonucleosides), we performed NMR analysis.

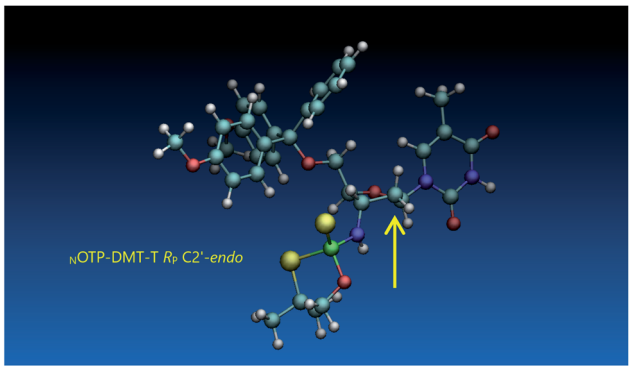

Fig. 5 Visualization of the lowest energy conformer of R_P-**5T** (the C2′-*endo* atom is marked with an arrow). The data were obtained using the Gaussian 16 package. Heteroatom labeling: P-green, O-red, S-yellow, N-navy blue.

Unexpectedly, the recorded 2D ^{1}H–^{1}H COSY and ^{1}H–^{13}C EDITED-HSQC spectra showed $^3J_{H1',H2'}$ = 6.5 Hz, which according to literature data[32] indicate a pseudorotation phase P = 90° or 195°. The former value is characteristic of a rare O4′-*endo* conformer, whereas the latter indicates a C2′-*endo* structure. To distinguish these options, a $^3J_{H3',H4'}$ value would be useful, but its measurement was significantly more complicated and neither analysis of the multiplicity of H3′ and H4′ signals nor attempts at simulation of the full spin system were successful. The molecular modeling experiments performed for R_P-**5T** (**5Ts**, slightly less effective than **5Tf** as shown in Table 2) showed that starting with C2′-*endo*, C3′-*endo*, or O4′-*endo* conformations the geometry optimization always ended at the

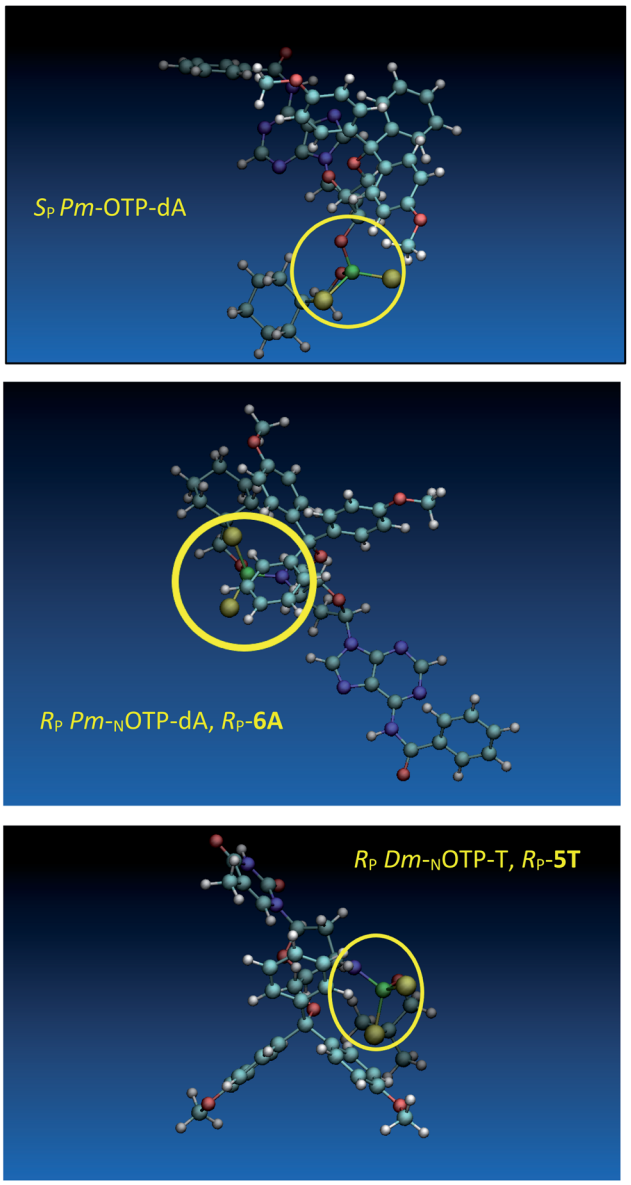

Fig. 6 Predicted by molecular modeling the lowest energy conformations of: S_P *Pm*-OTP-dA, an upper panel; R_P-**6A**, a middle panel; R_P-**5T**, a bottom panel. All three compounds are P-stereochemically equivalent (*vide supra*).

C2′-*endo* conformation (Fig. 5), characteristic of the OTP-N monomers.

Analogous calculations were performed for (S_P)-5′-*O*-DMT-*N*6-benzoyl-2′-deoxyadenosine-3′-*O*-(2-thio-4,4-pentamethylene-1,3,2-oxathiaphospholane) (S_P *Pm*-OTP-dA, slightly less reactive than the R_P counterpart), and (R_P)-5′-*O*-DMT-*N*6-benzoyl-3′-amino-2′,3′-dideoxy-adenosine-3′-*N*-(2-thio-4,4-pentamethylene-1,3,2-oxathiaphospholane) (R_P *Pm*-$_N$OTP-dA, R_P-**6A**, the least effective monomer as shown in Table 5). [Note: looking along the P–O3′ bond in S_P *Pm*-OTP-dA and along the P–N3′ bond in R_P-**6A**, despite of the opposite absolute configurations of phosphorus atoms (S_P *vs.* R_P), all other substituents attached to the P-atoms are positioned with similar spatial orientations, so that both compounds are P-stereochemically equivalent.] Independent of the implemented solvent (acetonitrile or chloroform), the results were very similar and showed (see the yellow circles) that the approach of the nucleophile along the P–O bond in S_P *Pm*-OTP-dA is virtually unrestricted (Fig. 6, an upper panel). Importantly, a similar marginally restricted approach is predicted for efficiently reacting **5Ts** (Fig. 6, a bottom panel). On contrary, in a poorly reacting C3′-*endo* (R_P)-3′-amino-2′,3′dideoxy-adenosine analog (a middle panel) such the approach is substantially blocked by the DMT propeller.

Indications of 'conformational clash'

In next three condensation experiments we used monomers of low coupling potency, *i.e.*, a **6Gf** + **6Gs** mixture. If $^{HO}T_{PS}$-d(G_{NPS}G)-**$** is condensed with an $_N$OTP-G monomer (Exp. #3), the product is formed in 49% yield (Fig. 3), while only 40% yield was noted for elongation of ^{HO}d(G_{NPS}G)-**$** (Table 5). If ^{HO}d($G_{NPS}$G)-**$** or ^{HO}d($G_{NPS}T_{PS}G_{NPS}$G)-**$** are elongated using an OTP-T monomer (C2′-*endo*) the efficacy is close to 90% (Exp. #4). If $^{HO}C^{(2'\text{-OMe})}{}_{PS}$T-**$** (the 2′-OMe unit exists in the C3′-*endo* conformation) reacts with an $_N$OTP-dG monomer (Exp. #5), *ca.* 50% efficacy is observed.

Important information comes from a paper by Hodgson and co-workers, which describes ^{1}H NMR conformational analysis of $T_{NP}{}^{S}T$ dinucleotide, which is an anionic *S*-alkyl phosphoramidothiolate compound bearing a 5′-deoxy-5′-thio-thymidine residue (^{S}T) at the 3′-end.[33] They found that the 3′-amino-2′,3′-dideoxy-ribose ring adopts the C3′-*endo* conformation, while the ring of the ^{S}T unit retains the C2′-*endo* conformation. Thus, the C3′-*endo* conformation is not transmitted downstream to the ^{S}T DNA unit and the preserved neighboring conformations C3′-*endo*/C2′-*endo* lead to the lowest overall energy of the $T_{NP}{}^{S}T$ system. This indicates that the C3′-*endo*/C2′-*endo* conformation of both nucleosides is energetically favored over the C3′-*endo*/C3′-*endo* conformation, which is observed in RNA/DNA hybrids. This observation may explain the greater reaction efficiency of $_N$OTP-N with a growing oligomer bearing the 5′-end DNA unit (the first coupling step and the result of Exp. #3). At this point, one can mention ^{DMT}dG$^{iBu}{}_{NPSMe}T_{OAc}$ (**10f**), which also adopted the C3′-*endo*/C2′-*endo* conformation (Fig. S8, ESI‡), and spontaneous crystallization of which indicates remarkably low energy of this system.

Table 6 NPS-Oligos synthesized at 1 μmol scale using the $_N$OTP-N and isolated by RP HPLC

Sequence	Code	$_N$OTP-N substrate	Yield[a] (%)	Amount[b] (OD)
d($G_{NPS}G_{NPS}$G)	**18f**	**6Gf**	17	0.5
	18s	**6Gs**	8	0.5
$T_{NPS}(T_{NPS})_4T$	**19f**	**5Tf**	37	4.2
	19s	**5Ts**	26	3.0
$T_{NPS}(T_{NPS})_5T$	**20m**	**5T**[c]	16	9.8
$T_{NPS}(T_{NPS})_8T$	**21m**	**5T**[c]	21	5.4
	21f	**5Tf**	17	7.5

[a] The yield calculated from the absorbance measured (at 504 nm) for the last dimethoxytrityl cation released compared to the initial value. [b] After double HPLC purification on a C18 reverse phase column. [c] An unresolved mixture of P-epimers.

Thus one can conclude that if the 5′-end segment of a growing oligomer ($^{HO}N_{NPS}$…-**$**, $^{HO}N^{LNA}{}_{PS}$…-**$** in Exp. #2, or $^{HO}C^{(2'\text{-OMe})}{}_{PS}$…-**$** in Exp. #5) and an incoming monomer ($_N$OTP-N or OTP-N^{LNA}) adopt the C3′-*endo* conformation there is a more crowded space around the phosphorus atom. This conformational 'clash' may result in a decrease of reaction rate that promotes additional side-reactions and may heighten the damaging effect of the aforementioned intrinsic lower reactivity of the thiophosphoramide $_N$OTP-N monomers compared to OTP-N. This decrease of coupling efficiency is much less severe if the incoming monomer exists in the C2′-*endo* conformation (Exp. #4 and relatively high reactivity of **5T**).

Attempts at solid phase synthesis of P-stereodefined NPS-oligo and chimeric NPS/PS and NPS/PO oligomers

The low repetitive yields encountered in the syntheses of $N_{NPS}N_{NPS}N$ with a random configuration of phosphorus atoms (Table 5) were confirmed (by the DMT^+ assay) by use of resolved P-epimers (see the column "Yield" in Table 6 for several examples). This circumstance rendered the syntheses of longer P-stereodefined NPS-oligo difficult. Also, to avoid extensive hydrolysis of phosphoramidothioate linkages upon treatment with 50% aqueous acetic acid[34] at the detritylation step, performed after the otherwise beneficial DMT-ON RP HPLC purification, the last step of the solid support synthesis included the use of an anhydrous 3% solution of DCA in methylene chloride for detritylation. In the case of short oligomers **18–20** (up to heptamers), careful RP HPLC purification furnished the products of satisfactory purity, as assessed by PAGE and MALDI-TOF MS analyses (data not shown). The earlier mentioned lower efficiencies of condensation for the purine monomers, as well as those for the slow-eluting compounds, were confirmed in the syntheses summarized in Table 6. Only homo-thymidine oligomers **19** and **20** were isolated in appreciable amounts, while the samples of **18f** and **18s** allowed only for MALDI-TOF MS analysis.

This modified approach was unsuccessful for the decamers **21** as neither RP nor IE HPLC purification provided products of acceptable purity. Therefore, the DMT-tagged oligomers **21** were isolated by means of RP HPLC using DMT-ON parameters. The

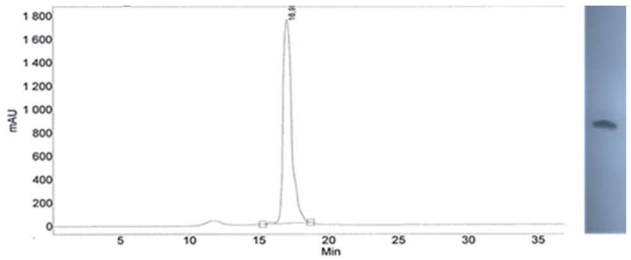

Fig. 7 Analysis of **21f** obtained from **5Tf**. (Left) An RP HPLC profile (DMT-OFF); (right): an electropherogram (20% PAGE).

final detritylation step was performed using 10% aqueous solution of dichloroacetic acid for 10 minutes, and the final RP HPLC purification was performed. The HPLC profile and the PAGE electropherogram recorded for **21f** are shown in Fig. 7, while the relevant ^{31}P NMR and MALDI-TOF MS spectra are shown in Fig. S8 (ESI).‡ Unfortunately, because of very low repetitive condensation yields, all attempts to synthesize **21** using **5Ts** were unsuccessful. This may indicate that **21m** obtained from unresolved **5T** predominantly contained the NPS linkages having the P atoms of R_P absolute configuration, but we were unable to confirm this assumption experimentally. Regretfully, at the time being, the field of antisense applications is inaccessible for uniformly modified P-stereodefined NPS-oligomers, although search for more effective conditions of condensation is going on. However, having resolved the problems with determination of the absolute configurations in the prepared monomers, one can use them in synthesis of precisely tailored probes (*e.g.* for enzymatic studies) bearing P-stereodefined NPS-units in a few preselected positions. As mentioned earlier, elongation of oligomers having at the 5′-end an N_{NPS} unit using an OTP-N monomer is more effective and a PS/NPS chimeric $T_{PS}dG_{NPS}T_{PS}dG_{NPS}dG$ oligomer (see observation #4 and Fig. 3, a middle plot) was obtained in 27% overall yield (assessed by the DMT$^+$ cation assay). This is an acceptable result when considering the known low efficacy of condensation (see Table 2) of *Pm*-$_N$OTP-dG.

Finally, we decided to explore the possibility of making chimeric NPS/PO oligomers. In an attempt to synthesize the 9-mer of the sequence 5′-$^{DMT}T_{PO}(T_{PO})_4(T_{NPS})_3$T-3′, the NPS-oligo fragment $T_{NPS}T_{NPS}T_{NPS}$T-**$** was assembled using the unresolved **4T**, with NEt_3 added in second and third coupling (Scheme S1, ESI‡). This $T_{NPS}T_{NPS}T_{NPS}$T-**$** core was intended to be elongated with the phosphate units using the phosphoramidite method of DNA synthesis. The standard protocol of the latter method could not be used, because past work in our group on the synthesis of PS/PO chimeras indicated that the anionic internucleotide phosphorothioate linkage is quantitatively converted to the phosphate derivative. This process occurs upon contact with an iodine–base–water solution (which is routinely applied to oxidize the just formed phosphite triester), as well as with many other reagents such as camphorsulfonyloxaziridine,[35] alkyl hydroperoxides[36] or peracids.[37] To a certain extent, this problem was resolved by *S*-alkylation of the PS-oligo core with 2-nitrobenzyl bromide to form the corresponding triester, which can be eventually deprotected with a thiophenolate anion. However, this process has only been optimized for d(N_{PS}N) dinucleotides.[38] Our later studies showed that the destructive PS → PO exchange in PS-oligo is avoided if the $P^{III} \rightarrow P^V$ conversion is performed using *t*-Bu-OOSiMe$_3$ (ref. 39) (0.33 M in CH_3CN, 30 min, room temperature).[40] In the present work, the ^{31}P NMR and MALDI-TOF MS measurements revealed that under these conditions the phosphoramidothioate linkage in $^{DMT}T_{NPS}T_{OAc}$ also remained unaffected (data not shown). The 9-nt $^{DMT}T_{PO}(T_{PO})_4(T_{NPS})_3$T-3′, was obtained in 42% yield as assessed from the DMT$^+$ cation assay. Its identity was confirmed by MALDI-TOF MS analysis (Fig. S9, ESI‡). Using 3*H*-1,2-benzodithiol-3-one 1,1-dioxide (a Beaucage reagent), ((dimethylamino-methylidene)amino)-3*H*-1,2,4-dithiazoline-3-thione (DDTT) or phenylacetyl disulfide to sulfurize the P atom in the phosphite triester linkage (formed after the phosphoramidite coupling step) the corresponding PS/NPS chimeras can be obtained.

Conclusions

In an attempt to synthesize P-stereodefined oligo(deoxyribonucleoside N3′ → O5′ phosphoramidothioate)s (NPS-) and chimeric NPS/PO- and NPS/PS-oligomers, 3′-*N*-(2-thio-1,3,2-oxathiaphospholane) derivatives of 5′-*O*-DMT-3′-amino-2′,3′-dideoxy-ribonucleosides ($_N$OTP-N), that bear a 4,4-unsubstituted, 4,4-dimethyl, or 4,4-pentamethylene substituted oxathiaphospholane rings, were synthesized. The four monomers **4A**, **5C**, **5T**, and **6G** were chromatographically separated into P-diastereomers, which were used in synthesis of dinucleotides $N_{NPS}N'$. One of the intermediate compounds, *i.e.*, $^{DMT}dG^{iBu}{}_{NPS}$-T_{OAc}, was converted into the *S*-Me derivative, which spontaneously crystallized. Analysis of the relevant diffraction data and the results of stereoselective HINT1 catalyzed hydrolysis of several P-diastereomerically pure $N_{NPS}N'$ provided an evidence that the earlier NMR based assignment of absolute configuration of the P-atom in $^{DMT}T_{NPSMe}T_{OAc}$ was incorrect. Mechanistic studies revealed that the relatively low repetitive yield observed during the synthesis of uniformly modified NPS-oligos is caused by a conformational 'clash' between adopting a C3′-*endo* conformation the 5′-end nucleoside (3′-amino-2′,3′-dideoxy-, but also 2′-OMe-, or LNA-nucleoside) of a growing oligomer and the incoming $_N$OTP-N monomer. This effect is less severe if the 5-end nucleoside (*e.g.* a DNA unit) adopts a C2′-*endo* conformation. Also, an NPS-core can be effectively elongated using the phosphoramidite approach giving rise to chimeric NPS/PO-oligomers.

Experimental section

Analytical equipment

^{1}H NMR and ^{31}P NMR spectra were recorded using Bruker AV-200 (200 MHz for ^{1}H) or DRX-500 (500.13 MHz for ^{1}H, 125.75 MHz for ^{13}C) instruments, with TMS or 85% H_3PO_4 used as external standards. High-resolution mass spectra (HRMS) were recorded using a Synapt G2 Si mass spectrometer (Waters) equipped with an ESI source and a quadrupole-time-of-flight mass analyzer. The measurements were performed in negative or positive ion modes, with the capillary and sampling cone

voltage set to 2.7 kV and 20 V, respectively. The source temperature was 110 °C. To ensure satisfactory accuracy, data were collected in a centroid mode and the readings were corrected during acquisition using leucine enkephalin as an external reference (Lock-SprayTM), which generated the reference ions at *m*/*z* 554.2615 Da ($[M - H]^-$) in the negative ESI mode and at *m*/*z* 556.2771 Da ($[M + H]^+$) in a positive ESI mode. The data sets were processed using the MassLynx 4.1 software (Waters). The FAB-MS spectra (13 keV, Cs^+) were recorded on a Finnigan MAT 95 spectrometer, in positive and negative ion modes. MALDI-TOF MS analyses of oligonucleotides were performed using a Voyager-Elite instrument (PerSeptive Biosystems Inc., Framingham, MA) operating in the reflector mode with the detection of negative ions. All UV absorption measurements were carried out in a 1 cm path-length cell, using a double beam spectrophotometer (CINTRA 10e, GBC, Dandenong, Australia), equipped with a silicon photo-diode detector.

Deprotected dinucleoside (N3′→O5′) phosphoramidothioates were isolated using a binary Varian HPLC system, consisting of two PrepStar 218 pumps and a ProStar 325 UV/VIS detector set at 260 nm. A reverse phase HPLC column (PRP-1, C18, 7 μm, 305 × 7 mm, Hamilton, Reno, NV) was eluted with a gradient of CH_3CN (1% min^{-1}) in 0.1 M TEAB (pH 7.3) at a 2.5 mL min^{-1} flow rate.

Analytical RP HPLC runs were performed using a Kinetex® 5 μm column 100 Å (4.6 × 250 mm, Phenomenex) at a 1 mL min^{-1} flow rate, buffer A, 0.05 M TEAB pH 7.5; buffer B, 40% CH_3CN in 0.05 M TEAB; a gradient 0 to 40% B over 30 min.

X-ray data were collected on a Bruker APEX III D8 Venture dual microsource system using phi and omega scans with graphite monochromatic Cu Mo Kα (λ = 1.54178 Å) radiation.

Materials

Silica gel chromatography media were supplied by MERCK. TLC silica gel 60 plates were used for routine analyses, while HPTLC silica gel 60 plates were used for the assessment of the chromatographic separability of P-diastereomers of the oxathiaphospholane derivatives; all plates contained a UV F_{254} indicator. Silica gel 60, 200–300 mesh, was used for routine open column chromatographic purification. Protected 3′-amino-2′,3′-dideoxy-ribonucleosides were purchased from Carbosynth Limited (Compton, United Kingdom) or Pharma Waldhof (Germany). 2-Chloro-1,3,2-oxathiaphospholane and its 4,4-substituted analogs were prepared according to the published methods.[4b] Acetonitrile (HPLC grade) used in the syntheses of oligonucleotides was dried over 3 Å molecular sieves until the residual moisture content dropped below 10 ppm (by Karl-Fischer coulometry).

Phosphitylation/sulfurization of 5′-*O*-DMT-nucleobase-protected 3′-amino-2′,3′-dideoxy-ribonucleosides with 2-chloro-1,3,2-oxathiaphospholane or its 4,4-substituted analogs – a general procedure

To a suspension of 5′-*O*-DMT-nucleobase-protected 3′-amino-2′,3′-dideoxy-nucleosides (1 mmol, the 3′-amino analogs of dA^{Bz}, dG^{iBu}, T, or dC^{Bz}) and elemental sulfur (2 mmol) in dry pyridine (4 mL), appropriate 2-chloro-1,3,2-oxathiaphospholane compound (R = H or Me, or R,R = $-(CH_2)_5-$, 1.2 mmol)[4b] was added dropwise using a gas-tight Hamilton syringe. The mixture was stirred at room temperature until the nucleoside disappeared (*ca.* 3 h, monitored by TLC). The solvent was evaporated and the residue was dissolved in acetonitrile (5 mL). Excess sulfur was filtered off and the filtrate was condensed *in vacuo*. The product (a mixture of P-diastereoisomers) was isolated by "flash" silica gel chromatography (230–400 mesh) using a column eluted with a linear 0→3% gradient of methanol in chloroform containing 0.1% pyridine. The mixtures of P-diastereomers of **4–6** were isolated in good yield (49–88%).

Separation of the P-diastereomers of $_N$OTP-N 4–6

A solution of the appropriate monomer **4–6** in 1.0 mL of the eluent specified in Table 1 was applied to a silica gel column (200 g, 75 × 2 cm). The column was eluted with 300 mL of the eluent and fractions at 10–12 mL were collected and analyzed on HP TLC plates. Yields and ^{31}P NMR chemical shifts of the isolated P-epimers are given in Table 1.

"In solution" synthesis of $^{DMT}dG^{iBu}{}_{NPSMe}T_{OAc}$ (10)

To a solution of 5′-*O*-DMT-*N*2-isobutyryl-3′-amino-2′,3′-dideoxy-guanosine-3′-*N*-(2-thio-4,4-pentamethylene-1,3,2-oxathiaphospholane) (**6Gf**, 0.844 g, 1 mmol) in anhydrous acetonitrile (5 mL), a solution of 3′-*O*-acetyl-thymidine (0.284 g, 1 mmol) and DBU (0.182 g, 1.2 mmol) in anhydrous acetonitrile (3 mL) was added. After 3 h, the reaction mixture was concentrated under reduced pressure. The residue was applied on a silica gel column, which was eluted with a linear 0→30% gradient of methanol in chloroform with 1% of pyridine. The product was isolated in 83% yield (^{31}P NMR ($CDCl_3$): δ 58.53 ppm; FAB MS: *m*/*z* 999.4 $(M-1)^-$). To its solution in a mixture of anhydrous acetonitrile (4 mL) and pyridine (1 mL), *N*,*N*-diisopropylethylamine (646 mg, 5 mmol) was added, followed by methyl iodide (710 mg, 5 mmol). The mixture was kept at room temperature overnight and concentrated under reduced pressure. The residue was applied on a silica gel column, which was eluted with a linear 0→10% gradient of methanol in chloroform containing 0.2% of pyridine. The triester was obtained in 63% yield (^{31}P NMR ($CDCl_3$): δ 36.06 ppm; ESI MS: *m*/*z* 1013.32, $(M-1)^-$). It crystallized at room temperature from a 50 : 1 (v/v) $CHCl_3$/MeOH mixture containing 4% of pyridine.

Crystallographic analysis of compound 10

Data sets were corrected for Lorentz and polarization effects as well as absorption. The criterion for observed reflections is $I > 2\sigma(I)$. Lattice parameters were determined from least-squares analysis and reflection data. Empirical absorption corrections were applied using SADABS.[41] structures were solved by direct methods and refined by full-matrix least-squares analysis on F^2 using X-SEED[42] equipped with SHELXT.[43] All non-hydrogen atoms were refined anisotropically by full-matrix least-squares on F^2 using the SHELXL[44] program. H atoms attached to oxygens were located in difference Fourier maps and refined isotropically with independent O–H distances. The remaining H

atoms were included in idealized geometric positions with $U_{iso} = 1.2U_{eq}$ of the atom to which they were attached ($U_{iso} = 1.5U_{eq}$ for methyl groups). Molecular configurations were compared to estimated Flack parameters.[45] The acetate group and one of the methanol solvate molecules exhibit two-part disorder with occupancies refined to 64 : 36 and 53 : 47, respectively. One of the methoxy groups exhibits three-part disorder with occupancies refined to 40 : 37 : 23. These disordered groups were refined with a mixture of restraints to approximate idealized geometries.

HINT1 catalyzed cleavage of the $N_{NPS}N'$ 11–17

The human Hint1 (HINT1) protein was expressed from the plasmid pSGA02 (ref. 46) in an *E. coli* strain BL 21* and was purified using AMP-agarose (Sigma-Aldrich) affinity chromatography according to the published procedure.[27] The homogenous enzyme preparations were dialyzed against 20 mM Tris and 150 mM NaCl buffer (pH 7.5), and the resultant solutions were concentrated to a protein concentration 10 mg mL^{-1} and stored at −80 °C.

For the hydrolysis of **11–17**, to the 50 μM solutions of the substrates prepared in 20 mM HEPES-Na, 0.5 mM $MgCl_2$ buffer (pH 7.2) HINT1 (1–13 μg, with the intention to provide rate of hydrolysis in pmol min^{-1} μg^{-1} protein) was added and the reaction mixtures (of total volume 20 μl) were incubated for 30–120 min at 37 °C. Then, the reaction mixtures were quenched by cooling on ice and analyzed by RP HPLC on a Kinetex column (5 μm C18, 100 Å, 250 × 4.6 mm; Phenomenex) with mobile phases A: 0.05 M TEAB pH 7.5; and B: 40% CH_3CN in 0.05 M TEAB delivered in a gradient from 0% to 17% B over 15 min, at a flow rate of 1 mL min^{-1}. Quantification was performed by integration of peaks of the substrate and products (including desulfured phosphate species) taking into account the number of chromophores in them. As the reference compounds appropriate nucleoside 5′-*O*-phosphorothioates and 5′-*O*-phosphates (dAMPS/dAMP, dGMPS/dGMP, TMPS/TMP) and 3′-amino-2,3′-dideoxy-nucleosides were used. Each experiment was performed in at least triplicate.

Introduction of N3′→O5′ phosphoramidothioate units during solid-phase synthesis of oligonucleotides

Syntheses were carried out manually using CPG-support, to which a 5′-*O*-DMT-nucleoside unit (1 μmol loaded) was attached with the succinyl-sarcosinyl type linker. A single cycle of chain elongation consisted of the following steps: (1) detritylation [3% dichloroacetic acid in methylene chloride (5 mL); 120 s]; (2) wash [acetonitrile (5 mL), methylene chloride (5 mL)] + drying; (3) coupling [a solution of $_N$OTP-N (20 μmol) and DBU (50 μmol) (+50 μmol of NEt_3 for $_N$OTP-T) in 0.15 mL of acetonitrile, freshly premixed; 900 s]; (4) wash [acetonitrile (5 mL), methylene chloride (5 mL)] + drying; (6) capping, [acetic anhydride/DMAP/2,6-lutidine/tetrahydrofuran (0.15 mL), 120 s]; (7) wash [acetonitrile (5 mL), methylene chloride (5 mL)] + drying.

The coupling efficiency was controlled by measurement of the DMT^+ absorption at 504 nm. The cleavage from the support and nucleobase deprotection were performed with 30% NH_4OH_{aq} at 55 °C for 8 h. Because post-synthetic detritylation with aqueous acetic acid would destroy the oligomer, after the oligonucleotide chain assembly was completed the "on-instrument" detritylation step was executed. Alternatively, after RP HPLC purification of DMT-tagged oligomers, the DMT group was removed with 10% aqueous solution of dichloroacetic acid for 10 minutes. All oligomers were purified by RP HPLC (a DMT-OFF procedure) and MALDI-TOF MS gave satisfactory results.

Molecular modeling

All calculations have been performed using a Gaussian 16 (G16) package.[31] In the calculations aimed at comparison of (S_P)-5′-*O*-DMT-*N*6-benzoyl-2′-deoxyadenosine-3′-*O*-(2-thio-4,4-pentamethylene-1,3,2-oxathiaphospholane) and (R_P)-5′-*O*-DMT-*N*6-benzoyl-3′-amino-2′,3′dideoxy-adenosine-3′-*N*-(2-thio-4,4-pentamethylene-1,3,2-oxathiaphospholane) (presented in Fig. 6), convergence to 10^{-8} in the energy and to 10^{-6} in the density matrix was used. An ultrafine grid with 75 radial shells and 302 angular points was employed. The geometry was optimized without any symmetry restrictions. The geometries of the compounds were generated *de novo* using multiple starting conformations and minimized using the polarizable continuum model (PCM) of the solvent. In two experiments acetonitrile and chloroform were set as the solvent with the standard parameter of dielectric constant ε of 35.7 and 4.7, respectively.[47] Optimizations were performed using the hybrid Hartree–Fock/Density Functional Theory (HF/DFT) method PBE0 (named also as PBE1PBE)[48] and the 6–311++G** basis set.[49] Each stationary point was characterized by calculating the harmonic vibration frequencies in order to verify that they have no imaginary frequency. Only the lowest energy structures were taken for the further evaluation.

Conflicts of interest

There are no conflicts to declare.

Acknowledgements

The authors thank Dr Wojciech J. Stec and Dr Sergei Gryaznov for encouraging and helpful discussions which prompted us to launch the project. This work was financially supported by statutory funds of Centre of Molecular and Macromolecular Studies, Polish Academy of Sciences, Łódź, Poland, and by National Centre of Science, Poland, grant UMO-2015/19/B/ST5/03116 to P. G. The support of X-ray instrumentation by the NSF-MRI grant CHE1827313 (to K. A. W.) is gratefully acknowledged. The computational resources were partially provided by the Polish Infrastructure for Supporting Computational Science in the European Research Space (PL-GRID).

Notes and references

1 P. C. Zamecnik and M. L. Stephenson, *Proc. Natl. Acad. Sci. U. S. A.*, 1978, **75**, 280; J. Kurreck, *Eur. J. Biochem.*, 2003, **270**,

1628; R. Kole, A. R. Krainer and S. Altman, *Nat. Rev. Drug Discovery*, 2012,, **11**, 12.

2 (*a*) F. Eckstein, *Antisense Nucleic Acid Drug Dev.*, 2000, **10**, 117; (*b*) P. Guga and M. Koziołkiewicz, *Chem. Biodiversity*, 2011, **8**, 1642; (*c*) F. Eckstein, *Nucleic Acid Ther.*, 2014, **24**, 374; (*d*) D. E. Volk and G. L. R. Lokesh, *Biomedicines*, 2017, **5**, 41; (*e*) X. Shen and D. R. Corey, *Nucleic Acids Res.*, 2018, **46**, 1584.

3 A. Wilk and W. J. Stec, *Nucleic Acids Res.*, 1995, **23**, 530.

4 (*a*) W. J. Stec, B. Karwowski, M. Boczkowska, P. Guga, M. Koziołkiewicz, M. Sochacki, M. Wieczorek and J. Błaszczyk, *J. Am. Chem. Soc.*, 1998, **120**, 7156; (*b*) P. Guga and W. J. Stec, in *Current Protocols in Nucleic Acid Chemistry*, ed. S. L. Beaucage, D. E. Bergstrom, G. D. Glick and R. A. Jones, John Wiley and Sons, Hoboken, N.J., 2003, p. 4.17.1.

5 A. Wilk, A. Grajkowski, L. R. Phillips and S. L. Beaucage, *J. Am. Chem. Soc.*, 2000, **122**, 2149; N. Oka, M. Yamamoto, T. Sato and T. Wada, *J. Am. Chem. Soc.*, 2008, **130**, 16031; K. W. Knouse, J. N. deGruyter, M. A. Schmidt, B. Zheng, J. C. Vantourout, C. Kingston, S. E. Mercer, I. M. Mcdonald, R. E. Olson, Y. Zhu, C. Hang, J. Zhu, C. Yuan, Q. Wang, P. Park, M. D. Eastgate and P. S. Baran, *Science*, 2018, **361**, 1234; N. Iwamoto, D. C. D. Butler, N. Svrzikapa, S. Mohapatra, I. Zlatev, D. W. Y. Sah, Meena, S. M. Standley, G. Lu, L. H. Apponi, M. Frank-Kamenetsky, J. J. Zhang, C. Vargeese and G. L. Verdine, *Nat. Biotechnol.*, 2017, **35**, 845.

6 P. Guga, M. Boczkowska, M. Janicka, A. Maciaszek, S. Kuberski and W. J. Stec, *Biophys. J.*, 2007, **92**, 2507; P. Guga, M. Janicka, A. Maciaszek, B. Rębowska and G. Nowak, *Biophys. J.*, 2007, **93**, 3567; A. Maciaszek, A. Krakowiak, M. Janicka, A. Tomaszewska-Antczak, M. Sobczak, B. Mikołajczyk and P. Guga, *Org. Biomol. Chem.*, 2015, **13**, 2375.

7 M. Boczkowska, P. Guga and W. J. Stec, *Biochemistry*, 2002, **41**, 12483.

8 M. Boczkowska, P. Guga, B. Karwowski and A. Maciaszek, *Biochemistry*, 2000, **39**, 11057.

9 P. A. Frey and R. D. Sammons, *Science*, 1985, **228**, 541.

10 L. Benimetskaya, J. L. Tonkinson, M. Koziołkiewicz, B. Karwowski, P. Guga, R. Zelser, W. J. Stec and C. A. Stein, *Nucleic Acids Res.*, 1995, **23**, 4239.

11 A. Krieg, P. Guga and W. J. Stec, *Oligonucleotides*, 2003, **13**, 491.

12 T. Inagawa, H. Nakashima, B. Karwowski, P. Guga, W. J. Stec, H. Takeuchi and H. Takaku, *FEBS Lett.*, 2002, **528**, 48.

13 (*a*) S. Gryaznov, T. Skorski, C. Cucco, M. Nieborowska-Skorska, C. Y. Chiu, D. Lloyd, J. K. Chen, M. Koziolkiewicz and B. Calabretta, *Nucleic Acids Res.*, 1996, **24**, 1508; (*b*) S. M. Gryaznov, *Biochim. Biophys. Acta*, 1999, **1489**, 131; (*c*) T. Skorski, D. Perrotti, M. Nieborowska-Skorska, S. M. Gryaznov and B. Calabretta, *Proc. Natl. Acad. Sci. U. S. A.*, 1997, **94**, 3966.

14 S. M. Gryaznov and J. K. Chen, *J. Am. Chem. Soc.*, 1994, **116**, 3143; J. P. Schrum, A. Ricardo, M. Krishnamurthy, J. C. Blain and J. W. Szostak, *J. Am. Chem. Soc.*, 2009, **131**, 14560; E. C. Izgu, S. S. Ohab and J. W. Szostak, *Chem. Commun.*, 2016, **52**, 3684.

15 S. M. Gryaznov, D. H. Lloyd, J.-K. Chen, R. G. Schultz, A. DeDionisio, L. Ratmeyer and W. D. Wilson, *Proc. Natl. Acad. Sci. U. S. A.*, 1995, **92**, 5798.

16 V. Tereshko, S. M. Gryaznov and M. Egli, *J. Am. Chem. Soc.*, 1998, **120**, 269.

17 R. Pruzan, K. Pongracz, K. Gietzen, G. Wallweber and S. M. Gryaznov, *Nucleic Acids Res.*, 2002, **30**, 559.

18 L. Kers, J. Stawiński and A. Kraszewski, *Tetrahedron*, 1999, **55**, 11579; K. Pongracz and S. M. Gryaznov, *Tetrahedron Lett.*, 1999, **40**, 7661; A. Asai, Y. Oshima, Y. Yamamoto, T. Uochi, H. Kusaka, S. Akinaga, Y. Yamashita, K. Pongracz, R. Pruzan, E. Wunder, M. Piatyszek, S. Li, A. C. Chin, C. B. Harley and S. Gryaznov, *Cancer Res.*, 2003, **63**, 3931.

19 W. J. Stec, A. Grajkowski, A. Kobylańska, B. Karwowski, M. Koziołkiewicz, K. Misiura, A. Okruszek, A. Wilk, P. Guga and M. Boczkowska, *J. Am. Chem. Soc.*, 1995, **117**, 12019.

20 B. Uznański, A. Grajkowski, B. Krzyżanowska, A. Kaźmierkowska, W. J. Stec, M. W. Wieczorek and J. Błaszczyk, *J. Am. Chem. Soc.*, 1992, **114**, 10197.

21 A. Krakowiak, R. Kaczmarek, J. Baraniak, M. Wieczorek and W. J. Stec, *Chem. Commun.*, 2007, 2163.

22 R. Kaczmarek, S. Kaźmierski, T. Pawlak, E. Radzikowska and J. Baraniak, *Tetrahedron*, 2016, **72**, 803.

23 F. Eckstein, P. M. J. Burgers and D. H. Hunneman, *J. Biol. Chem.*, 1979, **254**, 7476; F. Eckstein, P. M. J. Burgers, B. K. Sathyanarayana and W. Saenger, *Eur. J. Biochem.*, 1979, **100**, 585; S. J. Benkovic and F. R. Bryant, *Biochemistry*, 1979, **18**, 2825; F. Eckstein, B. V. L. Potter and B. Connolly, *Biochemistry*, 1983, **22**, 1369.

24 B. Karwowski, A. Okruszek, J. Wengel and W. J. Stec, *Bioorg. Med. Chem. Lett.*, 2001, **11**, 1001.

25 K. Jastrzębska, A. Maciaszek, R. Dolot, G. Bujacz and P. Guga, *Org. Biomol. Chem.*, 2015, **13**, 10032.

26 J. Martin, M. V. St-Pierre and J. F. Dufour, *Biochim. Biophys. Acta*, 2011, **1807**, 626.

27 P. Bieganowski, P. N. Garrison, S. C. Hodawadekar, G. Faye, L. D. Barnes and C. Brenner, *J. Biol. Chem.*, 2002, **277**, 10852.

28 M. Ozga, R. Dolot, M. Janicka, R. Kaczmarek and A. Krakowiak, *J. Biol. Chem.*, 2010, **285**, 40809.

29 T. Brown, C. E. Pritchard, G. Turner and S. A. Salisbury, *J. Chem. Soc. Chem. Commun.*, 1989, 891.

30 J. Baraniak, D. Korczyński and W. J. Stec, *J. Org. Chem.*, 1999, **64**, 4533.

31 M. J. Frisch, G. W. Trucks, H. B. Schlegel, G. E. Scuseria, M. A. Robb, J. R. Cheeseman, G. Scalmani, V. Barone, G. A. Petersson, H. Nakatsuji, X. Li, M. Caricato, A. V. Marenich, J. Bloino, B. G. Janesko, R. Gomperts, B. Mennucci, H. P. Hratchian, J. V. Ortiz, A. F. Izmaylov, J. L. Sonnenberg, D. Williams-Young, F. Ding, F. Lipparini, F. Egidi, J. Goings, B. Peng, A. Petrone, T. Henderson, D. Ranasinghe, V. G. Zakrzewski, J. Gao, N. Rega, G. Zheng, W. Liang, M. Hada, M. Ehara, K. Toyota, R. Fukuda, J. Hasegawa, M. Ishida, T. Nakajima, Y. Honda, O. Kitao, H. Nakai, T. Vreven, K. Throssell,

J. A. Montgomery Jr, J. E. Peralta, F. Ogliaro, M. J. Bearpark, J. J. Heyd, E. N. Brothers, K. N. Kudin, V. N. Staroverov, T. A. Keith, R. Kobayashi, J. Normand, K. Raghavachari, A. P. Rendell, J. C. Burant, S. S. Iyengar, J. Tomasi, M. Cossi, J. M. Millam, M. Klene, C. Adamo, R. Cammi, J. W. Ochterski, R. L. Martin, K. Morokuma, O. Farkas, J. B. Foresman and D. J. Fox. *Gaussian 16, Revision A.03*, Gaussian, Inc., Wallingford CT, 2016.

32 J. P. Marino, H. Schwalbe and Ch. Griesinger, *Acc. Chem. Res.*, 1999, **32**, 614.

33 L. P. Conway, S. Mikkola, A. C. O'Donoghue and D. R. W. Hodgson, *Org. Biomol. Chem.*, 2016, **14**, 7361.

34 M. Ora, M. Murtola, S. Ahoa and M. Oivanen, *Org. Biomol. Chem.*, 2004, **2**, 593.

35 T. Wada, A. Mochizuki, Y. Sato and M. Sekine, *Tetrahedron Lett.*, 1998, **39**, 7123.

36 Y. Hayakawa, M. Uchiyama and R. Noyori, *Tetrahedron Lett.*, 1986, **27**, 4191.

37 K. Ogilvie and M. J. Nemer, *Tetrahedron Lett.*, 1981, **22**, 2531.

38 B. Nawrot, B. Rębowska, K. Cieślińska and W. J. Stec, *Tetrahedron Lett.*, 2005, **46**, 6641.

39 G. M. Salamończyk, M. Kuźnikowski and E. Poniatowska, *Tetrahedron Lett.*, 2002, **43**, 1747.

40 E. Radzikowska and J. Baraniak, *Org. Biomol. Chem.*, 2015, **13**, 269.

41 G. M. Sheldrick, *SADABS (2016/2)—Program for Area Detector Absorption Corrections*, University of Göttingen, Göttingen, Germany, 2016.

42 L. J. Barbour, *J. Supramol. Chem.*, 2001, **1**, 189.

43 G. M. Sheldrick, *Acta Crystallogr., Sect. A: Found. Crystallogr.*, 2015, **71**, 3.

44 G. M. Sheldrick, *Acta Crystallogr., Sect. C: Struct. Chem.*, 2015, **71**, 3.

45 H. D. Flack, *Acta Crystallogr.*, 1983, **39**, 876.

46 S. Ghosh and J. M. Lowenstein, *Gene*, 1996, **176**, 249.

47 S. Miertus, E. Scrocco and J. Tomasi, *J. Chem. Phys.*, 1981, **55**, 117; J. Tomasi, B. Mennucci and R. Cammi, *Chem. Rev.*, 2005, **105**, 2999.

48 C. Adamo and V. Barone, *J. Chem. Phys.*, 1999, **110**, 6158.

49 R. Krishnan, J. S. Binkley, R. Seeger and J. A. Pople, *J. Chem. Phys.*, 1980, **72**, 650.

50 Z. Gunnur Dikmen, T. Ozgurtas, S. M. Gryzanov and B.-S. Herbert, *Biochim. Biophys. Acta*, 2009, **1792**, 240; B.-S. Herbert, G. C. Gellert, A. Hochreiter, K. Pongracz, W. E. Wright, D. Zielinska, A. C. Chin, C. B. Harley, J. W. Shay and S. M. Gryaznov, *Oncogene*, 2005, **24**, 5262.

51 E. H. Blackburn, *Mol. Cancer Res.*, 2005, **3**, 477; J. W. Shay and W. E. Wright, *Nat. Rev.*, 2006, **5**, 577; J. M. Y. Wong and K. Collins, *Lancet*, 2003, **362**, 983.